Trisodium 2-Hydroxypropane-1,2,3-Tricarboxylate Encapsulated Nanocontainer-Based Template-Free Electrochemical Synthesis of Multidimensional Copper/Copper Oxide Nanoparticles

Mona Saini, Nutan Rani, Asifa Mushtaq, Rini Singh, Seema Rawat, Manoj Kumar, and Kalawati saini

1 Introduction

Copper nanoparticles (NPs) are of great importance due to their wide application in anti-viral/antibacterial coatings [1–3], CO_2 adsorption [4–6], methanol oxidation [7], electronics [8], and sensor [9]. Copper is a good alternative to more costly metallic silver and gold nanoparticles and can be used for antibacterial, photocatalytic, and

M. Saini · N. Rani · K. saini (✉)
Department of Chemistry, Miranda House, University of Delhi, Patel Chest Marg, New Delhi 110007, India
e-mail: kalawati.saini@mirandahouse.ac.in

N. Rani
e-mail: nutan.rani@mirandahouse.ac.in

A. Mushtaq
Department of Botany and Microbiology, Garhwal University, H.N.B, Srinagar, Uttarakhand 241674, India

R. Singh
Graduate School of Engineering, Hiroshima University, 1-4-1 Kagamiyama, Higashi-Hiroshima 739-8527, Japan
e-mail: rini@hiroshima-u.ac.jp

S. Rawat
School of Life Sciences, Central University of Gujarat, Sector-30, Gandhinagar, Gujarat 382030, India
e-mail: seema.rawat@cug.ac.in

M. Kumar
Department of Physics, Malaviya National Institute of Technology, Jaipur, Rajasthan 302017, India

U. K. Mudali et al. (eds.), *Recent Trends in Electrochemical Science and Technology*, Springer Proceedings in Materials 15,
https://doi.org/10.1007/978-981-16-7554-6_18

biomedical applications. Also, copper nanoparticles have higher catalytic efficiency than other nanoparticles [10, 11]. The properties of copper nanoparticles can be controlled easily by changing the synthesis pathway. Copper nanoparticles have been synthesized using various routes like chemical reduction, biological and non-biological methods, chemical wet method (solvents thermal decomposition), green synthesis (surfactant-less), and other modified methods [12–16]. They can easily oxidize to form copper oxides. To avoid oxidation, these syntheses are performed in non-aqueous media at a low concentration of precursor and under an inert atmosphere either in nitrogen or in argon atmosphere.

Template-assisted electrochemical synthesis of semiconductor nanowires has been reported by Sisman et al. [17]. Lithographically patterned metallic nanowire electrodeposition (LPNE) has been reported by Menke et al. [18], which is an example of bottom-up electrochemical synthesis. Template-based electrochemical synthesis of copper (Cu) nanowires has been reported by Gupta et al. [19] and could sense CH_2Cl_2. Synthesis of copper oxide nanoparticles using carbon nanotubes as templates has been reported by Wu et al. [20]. Template-free synthesis of copper oxide has been carried out by using the precipitation method [22]. Simple template-free synthesis of $Cu(OH)_2$ and CuO nanostructures in a solution phase has been demonstrated by Mehdizadeh et al. [22]. Nanostructure and microstructures of polypyrrole have been synthesized by an electrochemical template-free process on a nickel (Ni) electrode [23].

In recent years, copper oxide nanostructured materials like nanorods [24], nanowires [25, 26], nanoribbons [27], nanobelts [28], and micro-sheets [29] are attracting the attention of researchers due to their potential biomedical applications. The clusters of metallic Cu have been prepared using reverse micelles as microreactors [30]. Heterostructures of CuO/polypyrrole (CuO/PPy) and CeO_2 polypyrrole (CeO_2/PPy) have been reported using the metal–organic decomposition (MOD) technique [31]. A variety of CuO nanostructures have been synthesized using high-temperature (at 393 K and 423 K) approaches like the hydrothermal method. The flower-like nanostructures of CuO have been synthesized using a hydrothermal method in a domestic microwave oven [32]. Electrochemical methods of preparation of Cu NPs have a low environmental impact and are cost-effective as reported by Saini et al. [33, 34]. Cu_2S nanoparticles have been electrochemically synthesized using cyclic voltammetry [35]. Potentiostatic electrochemical deposition (ECD) of copper sulfate solution within the nanochannels of porous anodic alumina templates has been used to fabricate copper nanowires [36]. Nanocomposites of CuO with multi-walled carbon nanotubes (MWCNT) and metallic Cu have been synthesized via electrochemical route [37, 38]. The synthesis of Cu_8O has been reported by Guan et al. [39]. The single-crystal X-ray structure of CuO has been determined at 196 K and room temperature by Asbrink et al. [40]. Electrochemical synthesis of copper oxide nanoparticles and nanorods has been reported in the literature [41, 42]. The synthesized nanorods have been studied for photocatalytic activity. Copper oxide (CuO) has been used for antibacterial application by Ren et al. [43]. Cu NPs have been studied for antibacterial activities against E. Coli by Raffi and coworkers [44]. Copper nanoparticles have also been reported as antibacterial agents by Mahmoodi

et al. [45]. The antibacterial activity of copper/C nanocomposites synthesized via the green route has been reported by Bhavyasree et al. [46].

In the electrochemical synthesis route, copper salt is not used; hence, pure materials can be synthesized without using any reducing agent. Also, one can synthesize crystalline materials using the direct electrochemical method. The advantages of this method are: (i) no need of washing synthesized material with alcohol and (ii) no need of annealing of sample for a long time. Thus, electrochemical synthesis follows the principle of green chemistry and is very promising for the synthesis of materials. The template-free electrochemical method is cost-effective, industrially feasible, and eco-sustainable process. In this paper, the synthesis of Cu/copper oxide nanoparticles (NPs) by electrochemical reduction using trisodium citrate as a capping agent is reported. The process is devoid of chemical reducing agents such as hydrazine hydrochloride, sodium borohydride, amino acids, cetyl trimethyl ammonium bromide, and N-benzyl-N-dodecyl-N-bis(2-hydroxyethyl) ammonium chloride. The NPs have been characterized using powder X-ray diffractometry (PXRD), scanning electron microscopy (SEM), energy dispersive spectroscopy (EDS), transmission electron microscopy (TEM), and X-ray photoelectron spectroscopy (XPS). To the best of the authors' knowledge, the developed protocol (electrochemical method at constant applied potential) for the synthesis of copper, cuprous oxide, and cupric oxide NPs is not reported in the literature. These nanoparticles can be used for photocatalytic and antibacterial activities. Herein the antimicrobial activities of the synthesized copper/copper oxide NPs against gram positive as well as gram negative bacteria are discussed.

2 Experimental

2.1 Chemicals and Reagents

All chemicals used for the synthesis were of analytical reagent grade. Trisodium citrate (TSC, 99%) was purchased from Merck Limited, India. The copper metal strip (99.9% pure, metal basis) was procured from Alfa Aesar, and a Pt strip (99.99%) used as a reference electrode was purchased from Sinsil International. All other chemicals were used as such without any further purification. AR grade NaOH was used to maintain the basic pH of the solution. A DC power supply (Keithley 2231A-30–3 triple channel) was used to synthesize the NPs.

2.2 Preparation of Copper/Copper Oxide Nanostructures

Nanoparticles of copper/copper oxide nanomaterials were prepared with various concentrations of TSC (50,100, 150, 200, 250 mM) and at various pH values of

reaction solutions 2.11, 4.22, 6.5, 7.8, 8.5, 13.11 with 2.55 mM of TSC to study the effect of pH and concentration of capping agent on the morphology of nanoparticles. The samples prepared at various pH values 2.1, 4.22, 7.8, and 8.5 with 2.55 mM of TSC and also with the above-mentioned other concentrations of TSC have been already reported in the literature [33]. So, herein the synthesis of copper/copper oxide nanostructures using 2.55 mM of TSC and at pH 13.11 is reported. The trisodium citrate (TSC) capped copper nanostructures (Cu and Cu_2O NPs) were synthesized via electrochemical route at pH 13.11, temperature of 373 K, and applied potential of 6.7 V. The concentration of TSC used was 2.55 mM. The pH 13.11 was maintained by the addition of 0.1 M of NaOH solution.

The electrochemical cell was formed by immersing the copper strip (anode, working electrode) and platinum strip (cathode, reference electrode) in 100 mL solutions of TSC. The TSC was used as the capping agent. Both electrodes were connected with a DC power supply, and the desired potential (6.7 V) was applied for a fixed time interval of two hours. The electrolysis of copper was carried out in the air for copper and copper oxide NPs using an electrochemical cell equipped with a magnetic stirrer at 450 rpm. The solution turned brownish red in 30 min after applying the set potential in the reaction setup which indicates the formation of Cu/Cu_2O NPs in the electrolyte solution. Then it turned blackish-red indicating the formation of all three types of NPs (Cu, Cu_2O, and CuO) in the electrolytic solution. The particles started accumulating or depositing at the Pt cathode when the potential was being applied. As soon as the power supply was stopped, the deposited $Cu/Cu_2O/CuO$ NPs got stripped off from the cathode in the form of precipitate and settled down at the bottom of the electrochemical cell. The precipitate was then filtered with Whatman filter paper number 42 and was washed several times with deionized water and then dried under vacuum. The powder was collected and used for further characterization.

2.3 Materials Characterization

Powder X-ray diffraction (PXRD) pattern of the dried powder was recorded using Bruker D8 Advance diffractometer equipped with Ni-filter and Cu Kα radiation. The data was collected in the 2θ range of 10–70° with a step size of 0.02° and a step time of 1 s. The surface morphology was studied by transmission electron microscopy (TEM) by using Tecnai G^2 F 20 TWIN TMPSeries microscope, Model FEG 200 kV. A carbon-coated copper grid was used for getting the TEM images of NPs. A freshly sonicated solution of 5 μL was spread with a 10 μL pipette on the carbon-coated side of the copper grid and dried under a bulb. Scanning electron microscopy (SEM) with energy dispersive spectroscopy (EDS) (JEOL JSM 6610 model no. at 20 kV) was used to obtain the morphology and composition of the synthesized powder. X-ray photoelectron spectroscopy (XPS, Omicron Nanotechnology, monochromatized Al, 1486.6 eV) was performed with XPS instrument having several features (ESCA + Omicron Nano Technology: Small spot XPS for high-speed depth profiling, Dual

Beam Charge Neutralization + Fully integrated Software Control and Automation, Rapid Quantification within Multipak or CASAXPS).

2.4 Antibacterial Activities

The antibacterial potential of $Cu/Cu_2O/CuO$ nanoparticles against the pathogens, viz. *Escherichia coli, Pseudomonas aeruginosa, Staphylococcus aureus, Streptococcus pneumoniae,* was evaluated by broth dilution method [47]. A stock solution of 2 mg/mL of nanoparticles was prepared by dispersing them in pre-sterilized deionized water by ultra-sonication. The varying concentrations ranging from 0.2 μg/mL to 200 μg/mL were prepared from stock solution and were added to the test tubes containing varying amounts of sterile Luria Bertani broth [48]. 50 μL of overnight culture (0.5 McFarland turbidity standards) of test pathogens was added to these tubes aseptically. The tubes were incubated at 37 °C for 24 h. The bacterial cultures without any test solution and the tubes with only sterile media were kept as positive and negative controls, respectively. The results were recorded by measuring the optical density of the inoculated broth at 600 nm. Minimum inhibitory concentration (MIC) was recorded as the lowest concentration of the test sample inhibiting the growth of the inoculated test pathogen.

3 Results and Discussion

During the electrochemical reduction, $Cu/Cu_2O/CuO$ is formed following the nucleation of the NPs by electrochemical reaction followed by the growth process. When the potential is applied, copper anode first gets oxidized into + 2 oxidation state.

$$Cu \rightarrow Cu^{2+} + 2e^{-} \tag{1}$$

This Cu^{2+} species in the presence of citrate capping agent and applied potential reduces back to Cu^{o} oxidation state (i.e., nucleation). The formation of copper oxides depends upon the applied potential, temperature, pH, and type of atmosphere (inert N_2/Ar/air). The formed nuclei are of different shapes of the NPs. The Cu^{o} nuclei then undergo a growth process to generate NPs. The growth process is controlled by the diffusion of growth species which in turn depends upon the concentration of trisodium citrate.

3.1 Powder X-ray Diffraction (PXRD) Analysis

The XRD pattern of the synthesized Cu/Cu_2O/CuO nanoparticles is shown in Fig. 1. The 2θ values at 43.65° and 50.43° correspond to (111) and (200) planes of cubic (face-centered) Cu (JCPDS, PDF, File No. 04–0836) phase. The other peaks at 2θ values of 32.49, 38.97, 47.29, 49.55, 51.40, 53.81, 58.39, 63.41, and 66.53° correspond to planes (110), (111), (-112), (-202), (112), (020), (202), (-113), and (022), respectively, match the monoclinic CuO (JCPDS, PDF, File No. 41–0254, 45–0937 and 80–1917) as reported in the literature [34, 35]. Herein, all three JCPDS file numbers are given for CuO nanoparticles. The other peaks at 2θ values of 33.08, 38.52,41.45, 44.74, 49.31, 51.67, 53.78, and 58.63° corresponding to planes (103), (004), (014), (220), (024), (105), (214), and (303) belong to copper oxide as reported by R. Guan [39] [(JCPDS, PDF, File No.78–1588)]. No impurity diffraction peaks have been detected which confirms the high purity of the product obtained by this method. The observation of diffraction peaks intensity for all the CuO nanoparticles indicates their high crystallinity. The intensity of peaks for primitive Cu_2O NPs at 2θ values 29.7°(110), 36.6°(111), 42.4°(200), and 61.4°(220) is found to be extremely low which shows that these NPs are less crystalline than the CuO NPs. It means PXRD analysis of the reaction products obtained at basic pH conditions does not contain pure CuO phase as reported by Nikam [49]. Based on XRD, it is clear that the peak intensity of CuO is found to be more as compared to Cu_2O and Cu NPs, respectively.

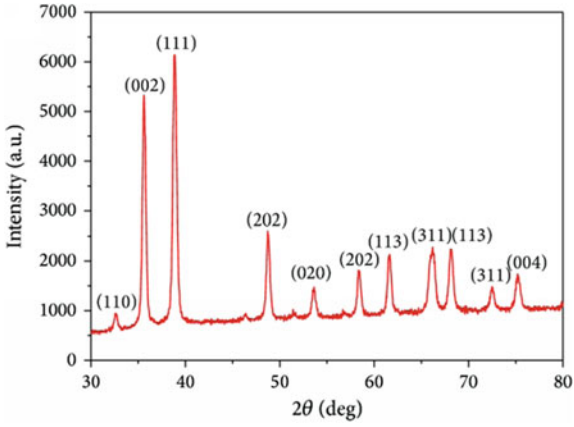

Fig. 1 Powder XRD pattern of Cu/Cu_2O/CuO nanoparticles with 2.55 mM trisodium citrate at 6.7 V, and at pH 13.11

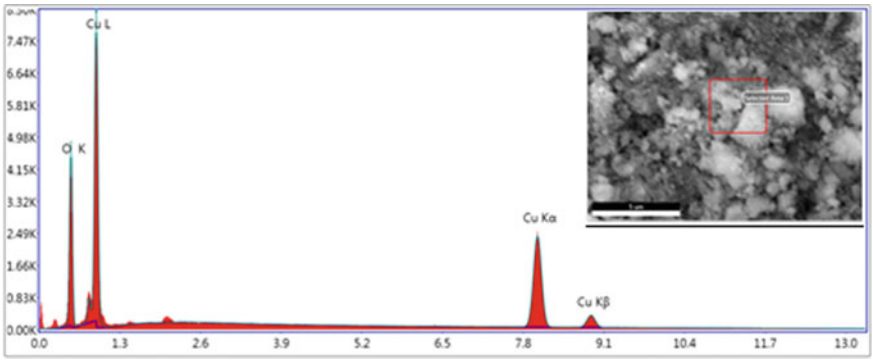

Fig. 2 EDS of the synthesized Cu/Cu_2O/CuO nanoparticles

3.2 EDS and TEM Analyses

The EDS of the synthesized nanoparticles is shown in Fig. 2. The EDS data confirmed the formation of copper/copper oxides nanoparticles. The atomic ratios of oxygen and copper were found to be 59.52 and 40.48%, respectively.

The sonicated aqueous solution of NPs was used for analyzing the morphology of the synthesized sample. Figure 3a–f shows the TEM images of Cu/Cu_2O/CuO NPs obtained at pH 13.11. These micrographs show different shapes of the nanoparticles such as leaf or feather, spherical, block-type, and rod-shaped. The leaf-shaped or feather-shaped particles have a length in the range of 5.24 μm and width in the range of 323 nm as shown in Fig. 3a. The block-type particles having one dimension as 135 nm as shown in Fig. 3b, c demonstrate the presence of all types of NPs with bigger sizes of rods having the dimension of 3.41 μm (length) and 125 nm (width).

The rod-shaped particles have a length of 205 nm and a width of 27.9 nm as shown in Fig. 3d. The spherical particles are also deposited on the surface of rods (Fig. 3d). The shape of spherical particles varies from 11.5 nm to 43.5 nm as shown in Fig. 3d–f and shows that some particles are agglomerated in a specific manner.

3.3 X-ray Photoelectron Spectroscopy (XPS) Analysis

XPS was used to determine the oxidation states and the surface chemical composition of the synthesized nanoparticles. Figure 4 shows the XPS spectra of the electrochemically synthesized Cu/Cu_2O/CuO NPs at applied potential of 6.7 V and pH of 13.11. The analysis of XPS peaks confirms the formation of a mixture of cuprous oxides (Cu_2O) and cupric oxides (CuO), respectively. Figure 4 demonstrates the deconvoluted XPS spectra of the Cu 2p core level. Doublet peaks positioned at binding energy of 932.43 eV and 952.72 eV in Cu_2O corresponding to Cu $2p_{3/2}$ and Cu $2p_{1/2}$, respectively. While the other doublet peaks are assigned corresponding to Cu $2p_{3/2}$

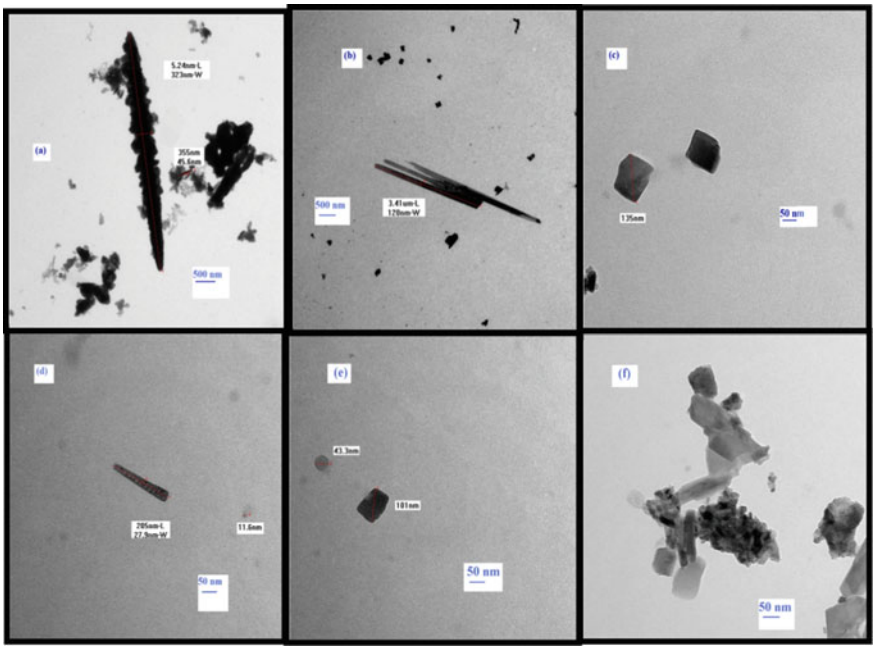

Fig. 3 TEM of $Cu/Cu_2O/CuO$ nanoparticles exhibiting various morphologies of the nanostructures

and Cu $2p_{1/2}$ in CuO at binding energy of 934.83 eV and 954.73 eV, respectively. The satellite peaks at 940.01 and 944.25 eV correspond to Cu $2p_{3/2}$ and Cu $2p_{1/2}$ in CuO and indicate the existence of an unfilled Cu 3d shell. The peak is assigned at a binding energy of 531.66 eV corresponding to O 1 s, and the calibration peak is obtained corresponding to C1s at binding energy of 288.50 eV and 284.97 eV, respectively. The obtained XPS data match well with the reported data in the literature [50–52]. Copper in CuO exists in the + 2 state with $3d^9$ configuration, while Cu_2O exists in + 1 state with $3d^{10}$ configuration as reported in the literature [53].

From the XPS results, we can estimate the ratio of Cu_2O and CuO on the basis of peak area. The fitting of high-resolution spectra of elements helps to quantify the ratio of oxidation states. The area ratio of CuO and Cu_2O is 7.3: 1. It is quite difficult to distinguish only Cu metal because of the similar binding energy of Cu and Cu(I) oxide. The peak position is in agreement with the reported literature [54, 55]. The % ratio of $Cu/Cu_2O/CuO$ in the mixture of synthesized material with XPS study was not possible.

Based on XPS peak-fit values of the Cu 2p core level measured on the surface of the synthesized NPs, the predominant phase was found to be CuO NPs and having adsorbed oxygen on the surface which can enhance its catalytic activity. This adsorbed oxygen can be used to enhance the photocatalytic and antibacterial activities.

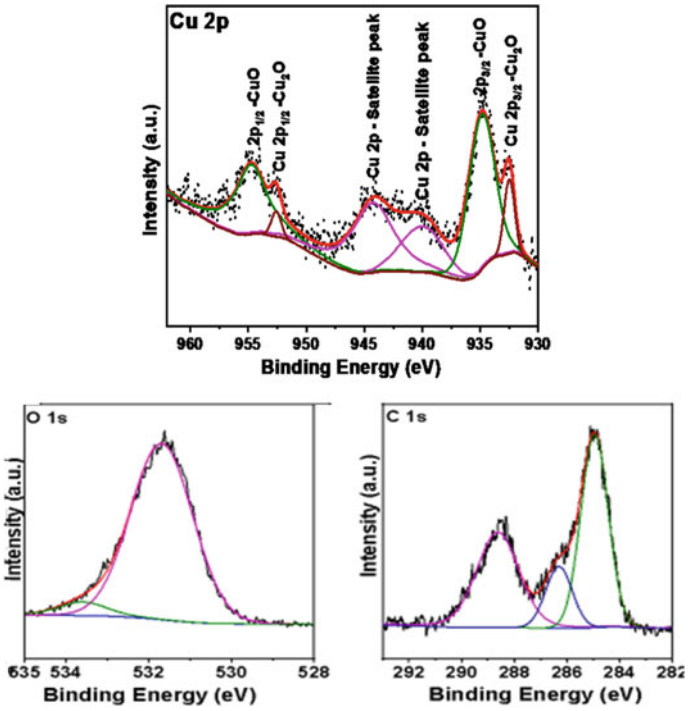

Fig. 4 Cu, O, and C XPS peaks of $Cu/Cu_2O/CuO$ nanoparticles synthesized from electrochemical route using 2.55 mM trisodium citrate at pH 13.11, 6.7 V at 373 K

3.4 Antibacterial Activity

It is well known that the CuO NPs show significant antibacterial activity against gram negative and gram positive bacteria. Herein, the antimicrobial activities of *Escherichia coli* (*E.Coli*) and *Pseudomonas Aeruginosa* have been studied. These are gram negative bacteria. The antimicrobial activities on *Staphylococcus Aureus* and *Streptococcus Pneumoniae* which are gram positive bacteria have also been studied. This study has been carried out using the broth dilution method. A higher value of minimum inhibitory concentration (MIC) indicates that a higher concentration of NPs is required to inhibit bacterial growth. The synthesized $Cu/Cu_2O/CuO$ nanoparticles do not affect the growth of *Pseudomonas Aeruginosa.* It means no inhibition (NI) of bacterial growth, as evident from Table 1. The MIC values were 155 μg/mL for *E.Coli* and 150 μg/mL for *Staphylococcus Aureus* as well as for *Streptococcus Pneumoniae.* These synthesized NPs show no inhibition on the growth of *Pseudomonas Aeruginosa.* These results are in good agreement with the reported results in the literature [56].

Table 1 Antibacterial activities of $Cu/Cu_2O/CuO$ nanoparticles with minimum inhibitory concentration (MIC, in μg/mL)

Isolates	$Cu/Cu_2O/CuO$ (MIC in μg/mL)
Escherichia coli (E. Coli)	155
Pseudomonas aeruginosa	No inhibition
Staphylococcus aureus	150
Streptococcus pneumoniae	150

4 Conclusions

The electrochemical reduction behavior of copper ions, as well as its nucleation and growth on a platinum electrode, has been studied in the aqueous solution of TSC. The copper electrode is the source of copper + 2 ions, and subsequently, it reduces to Cu at the platinum electrode and in a solution of 2.55 mM TSC having pH 13.11 in the electrochemical cell. In a basic medium, these Cu NPs again oxidize into Cu_2O and CuO, respectively. The PXRD and EDS analysis confirmed the formation of both types of oxides. The XPS analysis showed the peak area ratio of CuO and Cu_2O as 7.3: 1

Both electrode potential and temperature play an important role in tuning the nucleation and growth kinetics and also in controlling the final morphologies of copper nanoparticles. The obtained images from TEM reveal the exact shape and size of synthesized NPs. This is a special and unique case of one-step template-free synthesis, in which we have obtained four different morphologies of NPs. These synthesized NPs show very good antimicrobial activities against *E.Coli*, *Staphylococcus Aureus,* and *Streptococcus Pneumoniae.* The MIC values of $Cu/Cu_2O/CuO$ nanoparticles have been found from 150 μg/mL to 155 μg/mL for inhibiting the growth of the above-mentioned bacteria.

The electrochemical synthesis is a novel technique that is simple and environment-friendly than the conventional chemical reduction methods. Thus, the electrochemical synthesis is an ideal process as it consumes less energy and has a high output (yield 80–90%) and easy to control the process parameters.

Acknowledgements The authors thank Department of Chemistry, Indian Institute of Technology, for providing the facility for PXRD. The authors also wish to thank the Department of Physics, MNIT, Jaipur, India, for XPS analysis. The authors also wish to thank Kusuma School of Biological Science, the Indian Institute of Technology for providing the facility for TEM and the University of Delhi (USIC), for providing the facility for SEM with EDS analysis.

References

1. Lakshmanan M, Anumakonda VR, Gobi SK, Suchart S, Kumar J, Parameswaranpillai RS (2019) Preparation of cellulose/copper nanoparticles bionanocomposite films using a bioflocculant polymer as reducing agent for antibacterial and anticorrosion applications. Compos B

Eng 175:107177. https://doi.org/10.1016/j.compositesb.2019.107177
2. Jagaran K, Singh M (2021) Nanomedicine for COVID-19: Potential of copper nanoparticles. Biointerface Res Appl Chem 11(3):10716–10728. https://doi.org/10.33263/BRIAC113.1071610728
3. Raha S, Mallick R, Basak S, Duttaroy A (2020) Is copper beneficial for COVID- 19 patients? Med. Hypotheses 142. https://doi.org/10.1016/j.mehy.2020.109814
4. Smyrnioti M, Tampaxis C, Steriotis T, Ioannides T (2020) Study of CO_2 adsorption on a commercial CuO/ZnO/Al_2O_3 catalyst. Catal Today 357:495–502. https://doi.org/10.1016/j.cattod.2019.07.024
5. Larmier K, Liao WC, Tada S, Lam E, Verel R, Bansode A, Urakawa A, Vives C, Copéret C (2017) CO_2-to-methanol hydrogenation on zirconia-supported copper nanoparticles: Reaction intermediates and the role of the metal–support interface. Angew Chem 56:2318. https://doi.org/10.1002/anie.201610166
6. Bersani M, Gupta K, Mishra AK, Lanza R, Taylor SFR, Islam H, Hollingsworth N, Hardacre C, de Leeuw NH, Darr JA (2016) Combined EXAFS, XRD, DRIFTS, and DFT study of nano copper-based catalysts for CO_2 hydrogenation. ACS Catal 6(9):5823. https://doi.org/10.1021/acscatal.6b01529
7. Studt F, Behrens M, Kunkes EL, Thomas N, Zander S, Tarasov A, Schumann J, Frei E, Varley JB, Abild-Pedersen F, Nørskov JK, Schlögl R (2015) The mechanism of CO and CO_2 hydrogenation to methanol over Cu-based catalysts. Chem Cat Chem 7(7):1232. https://doi.org/10.1002/cctc.201590041
8. Sagadevan S, Murugasen P (2015) Electrical properties of copper oxide nanoparticles. Nano Res 30:1. https://doi.org/10.4028/www.scientific.net/JNanoR.30.1
9. Kang X, Mai Z, Zou X, Cai P (2007) A sensitive nonenzymatic glucose sensor in alkaline media with a copper nanocluster/multiwall carbon nanotube-modified glassy carbon electrode. Anal Biochem 363(1):143. https://doi.org/10.1016/j.ab.2007.01.003
10. Roudriguze JA, Lui P, Hrbek J, Evans J, Parez M (2007) Water gas shift reaction on Cu and Au nanoparticles supported on CeO_2(111) and ZnO(0001): intrinsic activity and importance of support interactions. Angew Chem Int Ed Engl 46(8):1329. https://doi.org/10.1002/anie.200603931
11. Ali ZI, Ghazy OA, Meligi G, Saleh HH, Bekhit M (2018) Radiation-induced synthesis of copper/poly(vinyl alcohol) nanocomposites and their catalytic activity. Adv Polym Technol 201:21675. https://doi.org/10.1002/adv.21675
12. Dang TMD, Le TTT, Fribourg-Blanc E, Dang MC (2011) The influence of solvents and surfactants on the preparation of copper nanoparticles by a chemical reduction method. Adv Nat Sci Nanosci Nanotechnol 2:025004. https://doi.org/10.1088/2043-6262/2/2/025004
13. Ghorbani HR (2014) Biological and non-biological methods for fabrication of copper nanoparticles. Chem Eng Commun 202(11):1463–1467. https://doi.org/10.1080/00986445.2014.950732
14. Zhong CJ, Mott D, Galkwoski J, Wang L, Luo J (2007) Synthesis of size-controlled and shaped copper nanoparticles. Langmuir 23(10):5740. https://doi.org/10.1021/la0635092
15. Khodashenas B, Ghorbani HR (2014) Synthesis of copper nanoparticles: an overview of the various methods. Korean J Chem Eng 31:1105–1109. https://doi.org/10.1007/s11814-014-0127-y
16. Wu S-H, Chen DH, Synthesis of high-concentration Cu nanoparticles in aqueous CTAB solutions. J Colloid Interface Sci 273:165. https://doi.org/10.1016/j.jcis.2004.01.071
17. Sisman I (2011) Template-assisted electrochemical synthesis of semiconductor nanowires. Chapter in book: Nanowires - Implementations and Applications, Source-InTech. https://doi.org/10.5772/20551
18. Menke EJ, Xiang C, Thompson MA, Yang LC, Penner RM (2006) Lithographically patterned nanowire electrodeposition. Nat Mater 5(11):914. https://doi.org/10.1038/nmat1759
19. Gupta J, Arya S, Singh A, Verma S, Sharma A, Singh B, Tomar A (2020) Template based electrochemical synthesis of copper (Cu) nanowires as CH_2Cl_2. Sensor Integr Ferroelectr 204:63. https://doi.org/10.1080/10584587.2019.1674990

20. Wu HQ, Wei XW, Shao MW, Gu JS, Qu MZ (2002) Synthesis of copper oxide nanoparticles using carbon nanotube as templates. Chem Phys Lett 364(1):152. https://doi.org/10.1016/S0009-2614(02)01301-5
21. Wahab R, Ahmad N, Alam M, Aldahmash AB, Abdulaziz A Al- Khedhairy (2016) Template free synthesis of copper oxide nanoparticles prepared via precipitation process. Asian J Chem 28(12):2622. doi:https://doi.org/10.14233/ajchem.2016.20029
22. Mehdizadeh R, Hasanzadeh M, Sanati S, Saghatforoush LA (2012) Simple template-free solution route for the synthesis of $Cu(OH)_2$ and CuO nanostructures and application for electrochemical determination three ß-blockers. J Exp Nanosci 9(8):763. https://doi.org/10.1080/17458080.2012.714479
23. Chebil S, Monod MO, Fisicaro P (2014) Direct electrochemical synthesis and characterization of polypyrrole nano- and micro-snails. ElectrochimActa 123:527. https://doi.org/10.1016/j.electacta.2014.01.058
24. Panigrahi S, Kundu S, Ghosh SK, Nath S, Praharaj S, Basu S, Pal T (2006) Selective one-pot synthesis of copper nanorods under surfactantless condition. Polyhedron 25(5):1263–1269. https://doi.org/10.1016/j.poly.2005.09.006
25. Wang X, Xiaofeng W, Yuan L, Huang K, Feng S (2017) Ultra-low reflection CuO nanowire array in-situ grown on copper sheet. Mater Design 113:297–304. https://doi.org/10.1016/j.matdes.2016.10.029
26. Kaur M, Muthe KP, Despande SK, Choudhury S, Sing JB, Verma N, Gupta SK, Yakhmi JV (2006) Growth and branching of CuO nanowires by thermal oxidation of copper. J Cryst Growth 289(2):670–675. https://doi.org/10.1016/j.jcrysgro.2005.11.111
27. Zhu CL, Chen CN, Hao LY, Hu Y, Chen ZY (2004) Template-free synthesis of $Cu_2Cl(OH)_3$ nanoribbons and use as sacrificial template for CuO nanoribbon. J Cryst Growth 263(1–4):473–479. https://doi.org/10.1016/j.jcrysgro.2003.11.003
28. Song X, Yu H, Sun S (2005) Single-crystalline CuO nanobelts fabricated by a convenient route. J Colloid Interf Sci 289:588. https://doi.org/10.1016/j.jcis.2005.03.074
29. Yang Q, Yan PX, Chang JB, Feng JJ, Yue GH (2007) Growth of bicrystal CuO microsheets from aqueous solution. Phys Lett A 361:493. https://doi.org/10.1016/j.physleta.2006.07.056
30. Lisiecki I, Pileni MP (1993) Synthesis of copper metallic clusters using reverse micelles as microreactors. J Am Chem Soc 115(10):3887–3896. https://doi.org/10.1021/ja00063a006
31. Galembeck A, Alves OL (1999) Planar heterostructures oxide/conducting polymer (CuO/polypyrrole and CeO/polypyrrole. Synth Met 102:1238. https://doi.org/10.1016/S0379-6779(98)01439-8
32. Volanti DP, Keyson D, Cavalcante LS, Simoes AZ, Joya MR, Longo E, Varela JA, Pizani PS, Souza AG, Volanti P, Keyson D, Cavalcante LS, Souza AG (2008) Synthesis and characterization of CuO flower-nanostructure processing by a domestic hydrothermal microwave. J Alloys Compd 459:537–542. https://doi.org/10.1016/j.jallcom.2007.05.023
33. Saini K, Devnani H, Bhat M, Ingole PP (2017) Anisotropic plasmonic copper/copper oxide nanostructures by DC electrophoretic dissolution of copper in water for plasmonic sensing of glucose. J Electrochem Soc 164(13):B674–B680. https://doi.org/10.1149/2.1391713jes
34. Saini K, Ingole PP, Bhatia SS, Rani N (2018) Rod-shaped copper (Cu, C_u2O) nano catalyst for the facile oxidation of methanol. Adv Mater Lett 9:36–41. https://doi.org/10.5185/amlett.2018.1714
35. Fotouhi L, Rezaei M (2009) Electrochemical synthesis of copper sulfide nanoparticles. Microchim Acta 167:247. https://doi.org/10.1007/s00604-009-0234-3
36. Gao T, Meng G, Wang Y, Sun S, Zhang L (2002) Electrochemical synthesis of copper nanowires. J Phys Condens Matter 14:355–363. https://doi.org/10.1088/0953-8984/14/3/306
37. Pandey P, Merwyn S, Agarwal GS, Pant SC (2012) Electrochemical synthesis of multi-armed CuO nanoparticles and their remarkable bactericidal potential against waterborne bacteria. J Nanopart Res 14(1):1–13. https://doi.org/10.1007/s11051-011-0709-0
38. Zhang QB, Hua YX (2014) Electrochemical synthesis of copper nanoparticles using cuprous oxide as a precursor in choline chloride–urea deep eutectic solvent: nucleation and growth mechanism. Phys Chem Chem Phys 16:27088. https://doi.org/10.1007/s11051-011-0709-0

39. Guan R, Hashimoto H, Kuo KH (1984) Electron-microscopic study of the structure of metastable oxides formed in the initial stage of copper oxidation. II Cu8O Acta Cryst B40:560–566. https://doi.org/10.1107/S010876818400269X
40. Asbrink S, Waskowska A (1991) CuO: X-ray single-crystal structure determination at 196 K and room temperature. J Phys Condens Matter 3:8173. https://doi.org/10.1088/0953-8984/3/42/012
41. Maria Starowicz M (2019) Electrochemical synthesis of copper oxide particles with controlled oxidation state, shape and size. Mater Res Express 6: 0850a3. 1088/2053–1591/ab239d
42. Mousali E, Zaanjanchi MA (2019) Electrochemical synthesis of copper (II) Oxides nanorods and their application in photocatalytic reactions. J Solid State Electrochem 23:925. https://doi.org/10.1007/s10008-019-04194-9
43. Ren G, Hu D, Cheng EW, Vargas-Reus MA, Reip P, Allaker RP (2009) Characterisation of copper oxide nanoparticles for antimicrobial applications. Int J Antimicrob Agents 33:587–590. https://doi.org/10.1016/j.ijantimicag.2008.12.004
44. Raffi M, Mehrwan S, Bhatti TM, Akhter JI, Hameed A, Yawar W, Masood ul Hasan M (2010) Investigations into the antibacterial behavior of copper nanoparticles against Escherichia coli. Ann Microbiol 60:75–80. https://doi.org/10.1007/s13213-010-0015-6
45. Mahmoodi S, Elmi A, Nezhadi HS (2018) Copper nanoparticles as antibacterial agents. Mol Pharm Org Process Res 6:1. https://doi.org/10.4172/2329-9053.1000140
46. Bhavyasree PG, Xavier TS (2020) Green synthesis of copper oxide/carbon nanocomposites using the leaf extract of Adhatoda vasica Nees, their characterization and antimicrobial activity. Heliyon 6:e03323. https://doi.org/10.1016/j.heliyon.2020.e03323
47. Garcia L (2010) Broth microdilution MIC Test, p 25–41. In Clinical Microbiology Procedures Handbook, 3rd edn. ASM Press, Washington, DC. https://doi.org/10.1128/9781555817435.ch5.2
48. Muniyan A, Ravi K, Mohan U, Panchamoorthy R (2017) Characterization and in vitro antibacterial activity of saponin-conjugated silver nanoparticles against bacteria that cause burn wound infections. World J Microbiol Biotechnol 33:147. https://doi.org/10.1007/s11274-017-2309-3
49. Nikam AV, Kashmir AA, Krishnamoorthy K, Kulkarni AA, Prasad BLV (2014) pH-dependent single-step rapid synthesis of CuO and Cu_2O nanoparticles from the same precursor. Cryst Growth Des 14:4329. https://doi.org/10.1021/cg500394p
50. Espinos JP, Morales J, Barranco A, Caballero A, Holgado JP, Gonzalez-Elipe AR (2002) Interface effects for Cu, CuO, and Cu_2O deposited on SiO_2 and ZrO_2. XPS determination of the valence state of copper in Cu/SiO_2 and Cu/ZrO_2 catalysts. J Phys Chem B 106:6921. https://doi.org/10.1021/jp014618m
51. Wang P, Ng YH, Amal R (2013) Embedment of anodized p-type Cu_2O thin films with CuO nanowires for improvement in photoelectrochemical stability. Nanoscale 5:2952. https://doi.org/10.1039/c3nr34012k
52. Ji JY, Shih PH, Yang CC, Chan TS, Ma YR, Yun Wu SY (2009) Spontaneous self-organization of Cu_2O/CuO core–shell nanowires from copper nanoparticles. Nanotechnology 21:045603. https://doi.org/10.1088/0957-4484/21/4/045603
53. Ghijsen J, Tjeng LH, Van Elp J, Eskes H, Westerink J, Sawatzky GA, Czyzyk MT (1988) Electronic structure of Cu_2O and CuO. Phys Rev B: Condens Matter 38:11322. https://doi.org/10.1103/PhysRevB.38.11322
54. Gupta A, Ramen Jamatia R, Patil RA, Ma Y-R, Pal AK (2018) Copper oxide/reduced graphene oxide nanocomposite-catalyzed synthesis of flavanones and flavanones with triazole hybrid molecules in one pot: a green and sustainable approach. ACS Omega 3:7288–7299. https://doi.org/10.1021/acsomega.8b00334
55. Gao Y, Yang F, Yu Q, Fan R, Yang M, Rao S, Lan Q, Yang Z, Zhenquan Y (2019) Three-dimensional porous $Cu@Cu_2O$ aerogels for direct voltammetric sensing of glucose. Microchim Acta 186:192. https://doi.org/10.1007/s00604-019-3263-6
56. Padil VVT, Cernik M (2013) Green synthesis of copper oxide nanoparticles using gum karaya as a biotemplate and their antibacterial application. Int J Nanomedicine 8:889–898. https://doi.org/10.2147/IJN.S40599